Seasonal, inter-annual and decadal drivers of tree and grass productivity in an Australian tropical savanna.

Seasonal, inter-annual and decadal drivers of tree and grass productivity in an Australian tropical savanna.

Journal:	*Global Change Biology*
Manuscript ID	GCB-17-1703.R1
Wiley - Manuscript type:	Primary Research Articles
Date Submitted by the Author:	02-Jan-2018

Complete List of Authors:	Moore, Caitlin; University of Illinois at Urbana-Champaign College of Liberal Arts and Sciences, Plant Biology; Monash University Faculty of Science, School of Earth, Atmosphere and Environment Beringer, Jason; University of Western Australia, School of Earth and Environment Donohue, Randall J; CSIRO Land and Water, Evans, Bradley; University of Sydney, School of Life and Environmental Sciences Exbrayat, Jean-François; University of Edinburgh, School of Geosciences Hutley, Lindsay; Charles Darwin University, School of Environmental and Life Sceinces Tapper, Nigel; Monash University Faculty of Science, School of Earth, Atmosphere and Environment

Keywords:	MODIS, Gross Primary Productivity, DIFFUSE model, random forest, carbon sequestration, southern oscillation index

Abstract:	Tree-grass savannas are a widespread biome and are highly valued for their ecosystem services. There is a need to understand the long-term dynamics and meteorological drivers of both tree and grass productivity separately in order to successfully manage savannas in the future. This study investigated the inter-annual variability (IAV) of tree and grass gross primary productivity (GPP) by combining a long-term (15 year) eddy covariance flux record and model estimates of tree and grass GPP inferred from satellite remote sensing. On a seasonal basis, the primary drivers of tree and grass GPP were solar radiation in the wet season and soil moisture in the dry season. On an inter-annual basis, soil water availability had a positive effect on tree GPP and a negative effect on grass GPP. No linear trend in the tree-grass GPP ratio was observed over the 15 year study period. However, the tree-grass GPP ratio was correlated with modes of climate variability, namely the Southern Oscillation Index. This study has provided insight into the long-term contributions of trees and grasses to savanna productivity, along with their respective meteorological determinants of IAV.

Title

Seasonal, inter-annual and decadal drivers of tree and grass productivity in an Australian tropical savanna.

Running Head

Savanna tree and grass productivity

Authors & Affiliations

Caitlin E. Moore[1,2]*, Jason Beringer[1,3], Randall J. Donohue[4,5], Bradley Evans[6,7], Jean-François Exbrayat[8], Lindsay B. Hutley[9], Nigel J. Tapper[1]

[1]School of Earth, Atmosphere and Environment, Monash University, Clayton, VIC, Australia, 3800

[2]Genomic Ecology of Global Change, Carl R. Woese Institute for Genomic Biology, University of Illinois, Urbana, IL, 61801, USA

[3]The UWA school of Agriculture and Environment, University of Western Australia, Crawley, WA, Australia, 6009

[4]CSIRO Land and Water, Canberra, Australia

[5]Australian Research Council Centre of Excellence for Climate System Science, Sydney, Australia

[6]Department of Environmental Sciences, The University of Sydney, Eveleigh, NSW, Australia, 2015

[7]Terrestrial Ecosystem Research Network Ecosystem Modelling and Scaling Infrastructure, The University of Sydney, Eveleigh, NSW, Australia, 2015

[8]School of GeoSciences and National Centre for Earth Observation, University of Edinburgh, Edinburgh, United Kingdom, EH9 3FF

[9]School of Environment, Research Institute for the Environment and Livelihoods, Charles Darwin University, Casuarina, NT, Australia, 0909

*Corresponding Author: caitlin@moorescience.com.au Ph: +1 217 208 1643

Key words

MODIS, GPP, DIFFUSE model, random forest, carbon sequestration, Southern Oscillation Index

Paper Type

Primary Research Article

Abstract

Tree-grass savannas are a widespread biome and are highly valued for their ecosystem services. There is a need to understand the long-term dynamics and meteorological drivers of both tree and grass productivity separately in order to successfully manage savannas in the future. This study investigated the inter-annual variability (IAV) of tree and grass gross primary productivity (GPP) by combining a long-term (15 year) eddy covariance flux record and model estimates of tree and grass GPP inferred from satellite remote sensing. On a seasonal basis, the primary drivers of tree and grass GPP were solar radiation in the wet season and soil moisture in the dry season. On an inter-annual basis, soil water availability had a positive effect on tree GPP and a negative effect on grass GPP. No linear trend in the tree-grass GPP ratio was observed over the 15 year study period. However, the tree-grass GPP ratio was correlated with modes of climate variability, namely the Southern Oscillation Index. This study has provided insight into the long-term contributions of trees and grasses to savanna productivity, along with their respective meteorological determinants of IAV.

Introduction

Savannas are a widespread biome characterised by a coexistence of trees and grasses that cover approximately 20 % of the global land surface (Scholes & Archer, 1997). They inhabit the continents of Australia, Africa, the Americas, Europe and Asia and are a vital source of food, timber products and income for a quarter of the world's human population (Mistry, 2001; Scholes & Archer, 1997; Shackleton et al., 2002). Savannas are also a key biome for terrestrial atmospheric carbon uptake via gross primary productivity (GPP), accounting for some 25 % of global GPP each year (Beer et al., 2010; Grace, José, Meir, Miranda, & Montes, 2006). However, plant respiration consumes approximately half of GPP, while heterotrophic respiration contributes to further carbon release to the atmosphere (Bonan, 2008; Chapin III, Matson, & Vitousek, 2011). Over longer timescales, disturbances such as grazing, land cover change (Bristow et al., 2016; Hutley et al., 2013; Hutley & Beringer, 2010), and fire (Beringer et al., 2015; Bond & Keeley, 2005; Bowman et al., 2010; Shi, Matsunaga, Saito, Yamaguchi, & Chen, 2015; Van Der Werf et al., 2010) return a portion of the sequestered carbon from GPP back to the atmosphere. Taking these factors into account, savanna ecosystems are still an important terrestrial sink of atmospheric carbon (0.5 – 2.0 Gt C y^{-1} globally; Grace, José, Meir, Miranda, & Montes, (2006); Scurlock & Hall, (1998)) and explain a large portion of inter-annual variability in the global land carbon sink (Ahlström et al., 2015; Poulter et al., 2014). Nevertheless, the seasonal, annual and inter-annual partitioning of this productivity between trees and grasses is still poorly understood for savannas (Moore et al., 2016; Whitley et al., 2011), which limits our ability to make informed decisions about savanna management into the future (Dyer & Smith, 2003; Scheiter, Higgins, Beringer, & Hutley, 2015; Shackleton et al., 2002; Walsh, Russell-Smith, & Cowley, 2014).

As the climate changes into the 21st century, there is uncertainty about how savanna ecosystems will respond (Scheiter & Higgins, 2009; Scheiter et al., 2015). Global climate

projections anticipate an increase in temperature and rainfall amount for most savanna regions as atmospheric carbon dioxide (CO_2) continues to rise (van Oldenborgh et al., 2013). Such changes to rainfall regimes will directly affect savannas due to the pivotal role of moisture availability as a driver of productivity (Beringer et al., 2011; Kanniah, Beringer, & Hutley, 2010, 2011; Whitley et al., 2011). Rising CO_2 poses an additional threat to savanna ecosystems from the effects of carbon fertilisation on savanna tree-grass structure. Tropical savanna grasses use a different photosynthetic pathway (C_4) when compared to the trees (C_3), which concentrates CO_2 at the photosynthetic reaction centres and provides grasses with a photosynthetic advantage over trees under current atmospheric conditions (Beerling & Osborne, 2006; Sage, 2004). Under higher atmospheric CO_2 tree productivity will be less limited by CO_2 availability, so they may experience a competitive advantage over the grasses as a result (Higgins & Scheiter, 2012). This phenomenon, where trees outcompete grasses, has been termed woody thickening, which is defined for savannas as an increase in woody standing biomass (Macinnis-Ng, Zeppel, Williams, & Eamus, 2011) and is likely to accelerate in coming decades (Browning, Archer, Asner, McClaran, & Wessman, 2008; Field, Lobell, Peters, & Chiariello, 2007; Scheiter & Higgins, 2009; Scheiter et al., 2015). Evergreen vegetation that persists year round will receive the greatest advantage from this CO_2 fertilisation effect (Donohue, McVicar, & Roderick, 2009), particularly in seasonally water limited and arid environments (Donohue, Roderick, McVicar, & Farquhar, 2013). Dynamic vegetation modelling in African (Scheiter & Higgins, 2009) and Australian (Scheiter et al., 2015) savannas has attributed increased atmospheric CO_2 and fire suppression as the primary drivers of this woody thickening.

To determine how woody thickening might change savanna tree-grass dynamics in the future, we need an understanding of how the trees and grasses have interacted in the past. We know that tree productivity declines from the wet to dry season in response to declining plant

available moisture and the resultant reduction in leaf area (Cernusak, Hutley, Beringer, Holtum, & Turner, 2011; Eamus, Hutley, & O'Grady, 2001; Eamus, Myers, Duff, & Williams, 1999; Eamus & Prior, 2001). Fire is also an important regulator of both ecosystem productivity (Beringer et al., 2003; Beringer et al., 2015; Beringer, Hutley, Tapper, & Cernusak, 2007) and the biomass proportion of trees to grasses. Fire is fuelled by dead grassy biomass and supresses juvenile woody recruitment to the overstory (Murphy, Russell-Smith, & Prior, 2010; Prior et al., 2006; Werner & Prior, 2013). Over longer timescales, macro-scale cyclical climate modes such as El Niño/La Niña, monsoonal systems and cyclones influence the amount of rainfall received in savanna regions (Hutley et al., 2013; Rogers & Beringer, 2017), which in turn has an effect on the productivity and tree-grass biomass of savanna ecosystems. Recent work from Moore et al., (2016) presents one of the first attempts at quantifying the relative contributions of productivity between trees and grasses using the eddy covariance technique. This study showed that in an Australian savanna, productivity was driven by both a strong seasonal input from the grasses and a comparatively consistent input from the trees. A model-based study at the same site as used by Moore et al., (2016), showed the importance of light limitation on tree-grass productivity (Whitley et al., 2011). While these two studies demonstrated the interaction of trees and grasses within the savanna ecosystem, both identified the need for longer term studies to explore the productivity dynamics of trees and grasses in more detail. In support of this, recent work from Ma, Baldocchi, Wolf, & Verfaillie, (2016) indicated that an ecosystem's carbon balance can respond slowly to climatological forcing, highlighting the need for more long term studies that explore such dynamics.

The combination of *in situ* monitoring and satellite remote sensing provides the tools necessary for establishing long term research studies that explore productivity dynamics within savanna ecosystems. In recent years, techniques have been developed using satellite

data to isolate tree and grass fractions in mixed ecosystems (Donohue et al., 2014; Zhou, Hill, Sun, & Schaaf, 2016); with time-series available from 2001 (i.e. MODerate resolution Imaging Spectroradiometer (MODIS)). Additionally, ecosystem monitoring at the Howard Springs savanna research site in Australia began in 1997 (Eamus, Hutley, & O'Grady, 2001) and the site now forms part of the Australian and New Zealand flux network (OzFlux), with continuous monitoring of fluxes since 2001 (Beringer et al., 2016). The continuous flux dataset, coupled with MODIS data, provides 15 years of information to explore the magnitude and underlying meteorological variables responsible for inter-annual variability in tree and grass productivity. Using this 15-year data set, we addressed the following research questions; (i) what are the most important meteorological factors that govern long-term productivity dynamics of trees and grasses in this savanna?; (ii) Is there any link between macro-scale climate modes and tree-grass GPP at our site?; and (iii) Can we detect woody thickening at our site? Understanding the importance of climatological factors for savanna tree-grass structure and productivity will contribute towards improvement of predictions of the impacts of climate change on this key global ecosystem.

Methods

Study site

The Howard Springs OzFlux and Fluxnet (AU-How) research site was used for this study, which is a mesic tropical savanna in the Northern Territory, Australia. Howard Springs (Fig. 1; c), and the wider Northern Territory region (Fig. 1; a & b), is classified as mixed 'savanna' and 'woody savanna' by the MODIS land cover product (MCD12Q1) that uses the International Geosphere-Biosphere Program (IGBP) defined land cover types (Friedl et al., 2002). The tree overstory comprises mostly *Eucalyptus miniata* and *E. tetrodonta*, with lesser abundant semi-, brevi- and fully deciduous species throughout, including *Terminalia*

ferdinandiana and *Erythrophleum chlorostachys* (Hutley, Beringer, Isaac, Hacker, & Cernusak, 2011; Williams, Myers, Muller, Duff, & Eamus, 1997). The understory consists mostly of C_4 grasses, including the annual *Sorghum intrans* and the perennials *Heteropogon triticeous* and *S. plumosum*, but also woody species including *Cycas armstrongii* and juvenile overstory species (Moore et al., 2016). The rainy season months from mid-October to mid-April account for 90-95 % of Howard Springs' mean annual rainfall of 1732 (± 44 SE, from 1941-2014) mm, (Australian Bureau of Meteorology (BoM), station ID: 014015, www.bom.gov.au). Mean daily air temperature (from 1941-2014) is very consistent throughout the year, with the monthly maxima ranging between 30.6 and 33.3 ˚C and minima between 19.3 and 25.3 ˚C (BoM, station ID: 014015, www.bom.gov.au). Soils in the region are weathered and nutrient poor red Kandosols (Isbell, 1996). Fire frequently occurs across the region, with recurrence rates between 1-5 years (Beringer et al., 2015; Jeremy Russell-Smith & Yates, 2007) and on longer timescales, cyclone activity also causes large disturbance (Hutley et al., 2013; Hutley & Beringer, 2010).

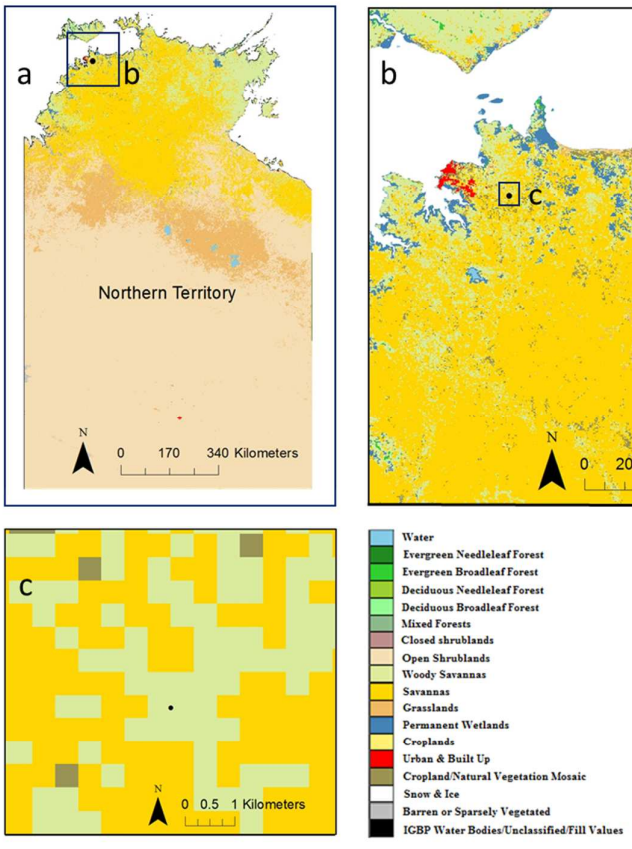

171

172

173 **Figure 1:** MODIS Land Cover Product (MCD12Q1) using the International Geosphere-
174 Biosphere Program (IGBP) classification system for a) the Northern Territory in
175 Australia, b) the northern-west region of the northern territory and c) the area directly
176 surrounding the Howard Springs OzFlux tower, with individual pixel resolution of
177 500 m (produced in ArcMap v10.1 using MODIS Land Cover data from (Gibson,
178 2015).

179

180 *Gross primary productivity from flux towers*

181 Eddy covariance flux towers were used in this study to estimate total ecosystem GPP, and its
182 overstory (tree) and understory (mostly grass) components, from measurements of net
183 ecosystem exchange (NEE). A flux tower at Howard Springs has been in continuous
184 operation since 2001 (Beringer et al., 2016; Eamus, Hutley, & O'Grady, 2001). In September
185 2012, an understory flux tower was installed to measure understory fluxes in conjunction
186 with the ecosystem tower (Moore et al., 2016). The understory tower was installed 10 m to
187 the west of the main ecosystem tower and recorded a representative footprint of the
188 understory fluxes within that of the main tower. This arrangement of total ecosystem and
189 understory measurements allowed for the separation of the overstory and understory carbon
190 fluxes. The understory tower has been extensively validated by Moore et al., (2016), where
191 details regarding the processing, quality assurance and quality control (QA/QC) of the flux
192 data, as well as the partitioning of net ecosystem exchange (NEE) into respiration and GPP,
193 and estimates of flux uncertainty can be found.

194 In brief, the principal eddy covariance instruments used in this study were an infrared gas
195 analyser (LI-7500, LI-COR Biosciences, Lincoln, NE) and a three dimensional sonic
196 anemometer (CSAT3, Campbell Scientific, Logan, UT). Both instruments measured at a rate
197 of 10 Hz and were averaged to 30-minute covariances of vertical wind velocity and scalars of
198 carbon, water and heat between the land surface and the atmosphere. In addition,
199 measurements of soil heat flux (HFT3, Campbell Scientific, Logan, UT), temperature (TCAV,
200 Campbell Scientific, Logan, UT) and moisture content (CS616, Campbell Scientific, Logan,
201 UT) were made along with net/short/long wave radiation (CNR4, Kipp and Zonen, Delft, NL),
202 air temperature and humidity (HMP45A, Vaisala, Vantaa, FI) and precipitation (TB3,
203 Hydrological Services, NSW, AU) on 30-minute averages.

204 The raw flux data were QA/QC'd to level 3 (L3) using the OzFluxQC (v2.9.4) standard
205 processing scripts (Isaac et al., 2017). Energy balance closure for the ecosystem tower 0.89
206 with an r^2 of 0.92 determined for daily data as per Leuning, van Gorsel, Massman, & Isaac,
207 (2012). We did not calculate energy balance closure for the understory tower due to the
208 difficulty in obtaining an accurate net radiation estimate. Instead, a co-spectral analysis was
209 performed on 10 Hz understory data to ensure the tower recorded turbulent fluxes during the
210 day (Moore et al., 2016). To gap fill the L3 flux data and partition NEE into respiration and
211 GPP, the Dynamic Integrated Gap filling and partitioning for OzFlux (DINGO) was used
212 (Beringer, Mchugh, Hutley, Isaac, & Kljun, 2017). This process was performed on 3 years of
213 understory data (2012-2015) and 15 years of ecosystem data (2001-2015). Once NEE was
214 gap-filled, model and random error was calculated based on McHugh et al. (2017), revealing
215 an error of 21.2 g C m^{-2} y^{-1} (4 % of NEE) for ecosystem and 25.8 g C m^{-2} y^{-1} (3.5 % of NEE)
216 for understory (Moore et al., 2016).

217

Modelling tree and grass GPP

To provide an estimate of tree and grass GPP over the past 15 years, we used the DIFFUSE model described by Donohue et al., (2014), which evaluates the fraction of tree and grass components based on their absorption of photosynthetically active radiation (PAR). The DIFFUSE model is formulated on the basis of Monteith's (1972) light use efficiency (LUE) model, estimating photosynthesis as a product of light absorbed (i.e. fraction of absorbed photosynthetically active radiation; APAR) along with the efficiency of its use (LUE, Equation 1):

$$GPP = C \times Fsd \times fPAR \times LUE \quad \text{Equation 1}$$

where fPAR refers to the fraction of PAR absorbed by an ecosystem, Fsd is shortwave radiation (J m^{-2} d^{-1}) and C is a constant that converts shortwave radiation into PAR ($C \approx 2.3 \times 10^{-6}$ mol J^{-1}). fPAR was calculated from the MODIS normalised difference vegetation index (NDVI) product (MOD13Q1) following Donohue et al., (2014). Fsd was calculated using meteorological grids of radiation at 0.05˚ resolution (downscaled to 250 m) and shuttle radar topographic mission (SRTM) elevation data at 1 s resolution to account for the effects of topography on Fsd. Donohue, McVicar, & Roderick, (2010) provide a detailed explanation of Fsd calculation. The DIFFUSE model estimates LUE as a function of maximum photosynthesis under direct radiation (i.e. A_x) and the diffuse (D_f) fraction of total incoming radiation. D_f varies depending on sky conditions from 1.0 under a fully overcast sky to 0.2 under clear sky conditions (Roderick, 1999). Taking this into account, the DIFFUSE model estimates LUE as (Equation 2):

$$LUE = 0.024D_f + 0.00061A_x \quad \text{Equation 2}$$

where A_x is the maximum rate of photosynthesis at the top of a canopy (μmol CO_2 m^{-2} s^{-1}) and the two constants (0.024 is unitless, 0.0061 has units of μmol PAR m^{-2} s^{-1}) are calculated from empirical observations of solar radiation across Australia (Roderick, 1999). The DIFFUSE model was parametrised at the continental scale for Australia using satellite remote sensing data (primarily from MODIS) and was validated against 12 OzFlux monitoring sites (Donohue et al., 2014). Equations 1 and 2 form the basis of the DIFFUSE model that provides data output in monthly resolution. Further information about DIFFUSE can be found in Donohue et al., (2014).

It should be noted that there may be some small differences between DIFFUSE and flux tower estimates because DIFFUSE evaluates the grass (and tree) components, whereas the flux tower measures the understory (grass plus some small shrubs). We have previously shown that in the savanna understory, grasses are the dominant vegetation during the wet season, with fire-suppressed saplings of the dominant woody tree and shrub species accounting for a modest fraction (~18 %) of annual GPP (Moore et al., 2016;, 2017). This contribution is particularly evident in the dry season when the senesced grasses do not contribute to GPP (Moore et al., 2016, 2017). The flux tower GPP estimates from the understory include this juvenile woody component, whereas the DIFFUSE model estimates were of C_3 (i.e. tree) and C_4 (i.e. grass) contributions. In addition, DIFFUSE was calculated from MODIS indices, whose temporal resolution is coarser than that of the flux towers. Therefore, we do not expect them to completely agree. From herein, we use tree and grass GPP to refer to the DIFFUSE model estimates and overstory and understory to refer to the flux tower estimates.

Despite the model-flux tower differences, the DIFFUSE grass estimates did capture the seasonality of the flux tower understory quite well, except that in preliminary simulations a model lag existed during the transition from wet to dry season (i.e. March to May). We

suspected this was due to the phenology of the C_4 annual grasses that dominate understory biomass not being fully captured by the DIFFUSE model. However, if it is assumed that the foliage cover of evergreen (or perennial) vegetation is reasonably invariant across seasons and that of annual (and ephemeral) vegetation is highly variable, the contribution of these two components to total foliage cover can be approximated. Donohue, McVicar, & Roderick (2009) developed such a method using a moving minimum approach. Due to the almost complete absence of deciduous vegetation in Australia, this approach has been shown to provide a reliable estimate of tree and grass foliage cover (Gill, Armston, Phinn, & Pailthorpe, 2006). Here, instead of applying this splitting method to foliage cover and using tree and grass cover to produce separate DIFFUSE-based estimates of tree and grass, we calculated ecosystem GPP using the DIFFUSE model and then applied the Donohue, McVicar, & Roderick, (2009) splitting algorithm to produce tree and grass GPP. This approach improved the ability of the DIFFUSE model to capture the seasonal dynamics of the understory flux tower (Figure 2) and these results are used in the following analyses. Tree GPP was then calculated as the difference between flux tower ecosystem GPP and DIFFUSE grass GPP as (Equation 3):

$$GPP_{Tree} = GPP_{Eco} - GPP_{Grass} \quad \text{Equation 3}$$

where GPP_{Eco} is the flux tower ecosystem GPP estimate and GPP_{Grass} is the DIFFUSE model GPP estimate. This method provided the closest fit with tree GPP estimates from the flux tower.

Determining the drivers of tree and grass productivity

Savanna ecosystem GPP varies over distinct time scales in response to meteorological and climatological conditions (Beringer et al., 2011; Kanniah, Beringer, & Hutley, 2010). Once we separated long-term ecosystem GPP into tree and grass estimates, we calculated anomaly values based on data grouped by water-year (i.e. July-June), to ensure the anomalies represented complete growing seasons. Tree and grass GPP anomalies, calculated as a change in yearly GPP (g C m^{-2} y^{-1}) from the 14 water-year mean, were compared against anomaly values using linear regressions for six primary meteorological drivers that are known to influence GPP (Kanniah et al., 2010). These drivers were also measured by the flux tower, and included solar radiation (Fsd, MJ m^{-2} y^{-1}), precipitation (Precip, mm y^{-1}), air temperature (Ta, ^{o}C), vapour pressure deficit (VPD, kPa), soil water storage (Sws, m^{3} m^{-3} y^{-1}) and rainy season length (RS, number of days per year).

To explore seasonality in the meteorological drivers of tree and grass GPP for each month of the year, we used the Random Forest machine learning technique described by Breiman, (2001) , and implemented using the Python Scikit-Learn module (Pedregosa et al., 2011). The Random Forest merges multiple mathematical decision trees (n = 1000) to split a population of dependent variables (i.e. GPP) as a function of a number of independent variables (i.e. meteorology). Each input variable was allocated an 'importance' value that was based on a tree-wise comparison of the explanatory power of the variables of each tree. Relative importance ranges from 0 – 1, with 0 indicating no importance and 1 indicating sole importance (Breiman, 2001; Exbrayat & Williams, 2015; López-Blanco et al., 2017). We tested the meteorological variables of Fsd, Precip, Ta, VPD and Sws on daily averaged data from 2001 to 2015 using Random Forests, and then grouped this data by month to investigate seasonal variability and IAV. Initial analysis used soil moisture at 10 cm, as this was available throughout the entire 15-year record. This surface Sws at 10 cm is quickly reduced

313 below field capacity in the dry season (Duff et al., 1997; Moore et al., 2016; Walker &
314 Langridge, 1997). To test the relative importance of deeper Sws for productivity, we added a
315 100 cm Sws measurement over a reduced time period (2008 to 2015), to account for
316 installation of the 100 cm sensor at the beginning of 2008. Given the shorter temporal length
317 of the 100 cm Sws time series, we did not use it in our IAV analysis.

318 Lastly, to explore long-term trends in the productivity of the trees and grasses, we calculated
319 a simple tree-grass GPP ratio (i.e. tree/grass) and plotted its annual anomaly values. Changes
320 in the tree-grass GPP ratio and anomaly values over time can provide an indication of the
321 potential for woody thickening at the site over the last 15 years. The anomaly values were
322 also compared against four key climate indices of climate variability that have been found to
323 perform well at describing long-term annual rainfall patterns at the Howard Springs site
324 (Rogers & Beringer, 2017). These four indices were the Southern Oscillation Index (SOI), the
325 Tasman Sea Index (TSI), the Indonesia Index (II) and the Australian Monsoon Index
326 (AUSMI). The SOI is a measure of the monthly mean sea level pressure difference between
327 Darwin and Tahiti and is commonly used as an indicator of El Niño and La Niña events
328 (Nicholls, 1991; Nicholls, 1989; Suppiah & Hennessy, 1996). The TSI and II are calculated
329 from sea surface temperatures, with the TSI from a region off the east coast of Australia (150
330 ^{o}E to 160 ^{o}E and 40 ^{o}S to 30 ^{o}S, (Murphy & Timbal, 2008)) and the II from a region
331 surrounding Indonesia (120 ^{o}E to 130 ^{o}E and 0 ^{o}N to 10 ^{o}S, (Nicholls, 1989; Schepen, Wang,
332 & Robertson, 2012)). The AUSMI provides an indication of the occurrence of the summer
333 monsoon that is a primary mechanism for delivering rainfall in northern Australia (Sturman
334 & Tapper, 2006). It is calculated from zonal wind velocity at 850 mb over a region of
335 Indonesia and north western Australia (110 ^{o}E to 130 ^{o}E and 5 ^{o}S to 15 ^{o}S, (Kajikawa, Wang,
336 & Yang, 2010)). Annual (i.e. water-year) anomaly values were calculated for each index
337 based on daily (TSI and II), monthly (SOI), or seasonal (AUSMI) data availability, which

were regressed against the annual tree-grass anomaly values to assess their correlations. Correlations were expressed as significant based on p-values <0.05.

Results

Long-term tree and grass GPP dynamics

To partition long-term ecosystem GPP at Howard Springs into tree and grass contributions, we first validated DIFFUSE model estimates of GPP against flux tower estimates for the 15-year ecosystem record and for the three years the understory tower was in operation (2012-2015). The DIFFUSE model performed well at capturing ecosystem flux tower seasonality in GPP over the 15-year study period (r^2 = 0.83; Figure 2, a), as well as the shorter 3-year subset (r^2 = 0.81; Figure 2, b). DIFFUSE also captured the seasonality of the grasses well, but slightly underestimated understory GPP in the dry season (r^2 = 0.82; Fig. 2, c). In contrast to the grasses, DIFFUSE performed less well at capturing the timing of tree GPP (r^2 = 0.39; Fig. 2, d). Given the overall strong fit between DIFFUSE and flux tower ecosystem GPP estimates, plus the strong fit of DIFFUSE with understory flux tower GPP, we used the grass DIFFUSE model to predict grass productivity over the 15-year ecosystem flux time-series.

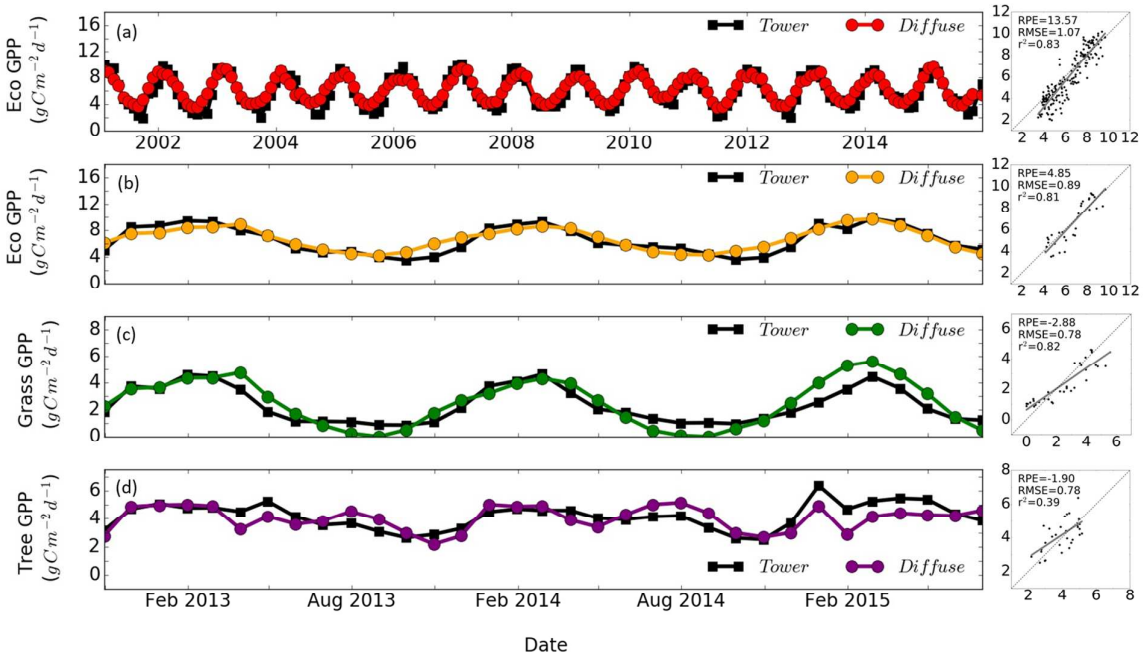

355

356 **Figure 2:** Time series and regression comparison of Howard Springs flux tower and
357 DIFFUSE model estimates of gross primary productivity (GPP, g C m^{-2} d^{-1}) for (a) 15
358 years (2001-2015) of ecosystem fluxes, and 3 years (September 2012 to June 2015) of
359 fluxes for (b) ecosystem, (c) grass and (d) tree. Regression plots show the line of best
360 fit (solid line), the 1:1 line (dashed line), the relative predictive error (RPE, %), the
361 root mean square error (g C m^{-2} d^{-1}) and the r^2 fit.

362

363 Using the DIFFUSE model grass GPP fraction, we then partitioned the long-term ecosystem
364 GPP tower estimate into monthly tree and grass contributions (Fig. 3). On an annual basis,
365 the grasses contributed an average of 41 % to ecosystem GPP, with a range from as low as
366 33 % in some years (i.e. 2010) and up to 50 % in other years (i.e. 2002 to 2003 and 2015, Fig.
367 3).

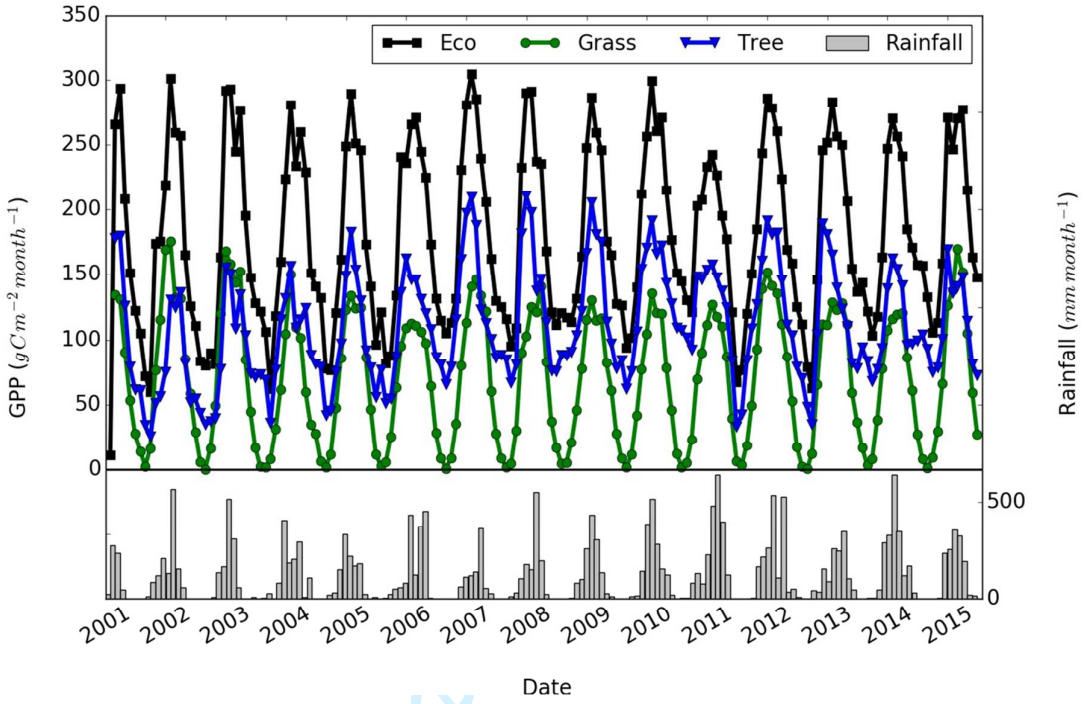

Figure 3: Long-term (15 year) ecosystem (Eco) gross primary productivity (GPP) flux tower time series, the partitioned (modelled) tree and grass GPP, plus rainfall, for the Howard Springs savanna site. Data are shown as monthly sums.

Seasonal and inter-annual drivers of tree and grass productivity

To analyse what meteorological variables are most important for seasonality of GPP, and if they differed between the trees and grasses, we used the Random Forest technique. This approach revealed that solar radiation (Fsd) was, not surprisingly, the most important (qualitative indication of co-variation) variable for determining wet season productivity for both the trees and grasses (Fig. 4; a & b). In contrast to the wet season, soil water availability (Sws) was the most important driver of tree and grass productivity in the dry season (Fig. 4; a & b). At the onset of the dry season (Apr-May), the upper soil layers have the highest importance for productivity, which switches to deeper soil moisture as the dry season

progresses (Fig. 4; e & f). This result is also reflected in the inter-annual analysis, showing that overall, Sws was the most important determinant of tree and grass GPP over the 15-year time series (Fig. 4; c & d).

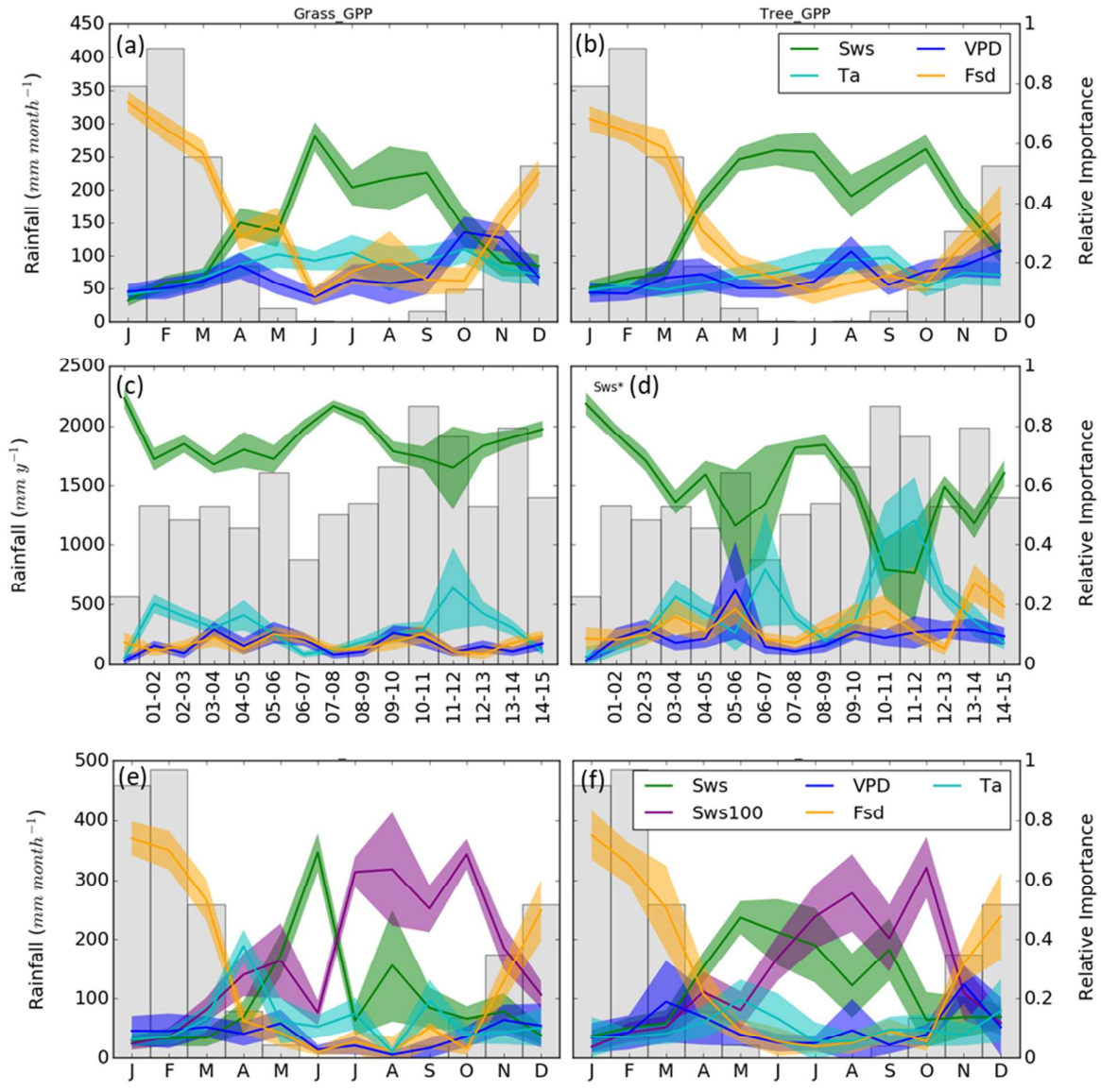

Figure 4: Meteorological drivers of monthly (a & b) and yearly (c & d) grass and tree gross primary productivity (GPP) from 2001 to 2015, plus a shorter temporal monthly time series (e & f) of tree and grass GPP from 2008 to 2015 at Howard Springs. Meteorological drivers include soil water storage at 10 cm (Sws), Sws at 100 cm

(Sws100), air temperature (Ta), vapour pressure deficit (VPD) and incoming solar radiation (Fsd). The bottom panel begins in 2008 due to the installation of the 100 cm Sws sensor in that year.

To explore IAV in tree and grass GPP, we calculated and plotted anomalies based on their respective 14 water-year (i.e. Jul-Jun) mean GPP values (Fig. 5). These plots showed that the GPP anomalies for trees appeared to increase over time, but that grass anomalies fluctuated around the mean. Included in Fig. 5 are anomalies for changes in the yearly sum of daily mean Fsd, Ta, Sws, soil temperature (Ts), and VPD, as well as changes in total annual rainfall. To determine which of these variables best described changes in tree and grass productivity inter-annually, we used a simple linear regression analysis. This approach showed that of the six variables, only Sws had a statistically significant influence on the IAV of the tree ($p = 0.003$) and grass ($p = 0.006$) GPP anomalies (Fig. 6), a finding also supported by the IAV Random Forest analysis (Fig. 4; c & d). Interestingly, the trees showed a positive correlation with increasing Sws (Fig. 6; e), while the grasses revealed a negative correlation with the increasing Sws anomalies (Fig. 6; k).

The key year that stands out in the anomalies of the 15-year monitoring period is 2010-2011, where the highest positive rainfall anomaly (Fig. 5; f) and greatest negative Fsd anomaly (Fig. 5; b) occurred. While the tree GPP anomaly was positive, it was not the highest recorded during this time period (Fig. 5; a), and the grass anomaly was negative, but not the most so (Fig. 5; e). Both tree and grass GPP anomalies became noticeably more positive in the year proceeding the 2010-2011 meteorological anomaly year (i.e. 2011-2012), while Fsd and rainfall were less variable than in 2010-2011 (Fig. 5 b & f).

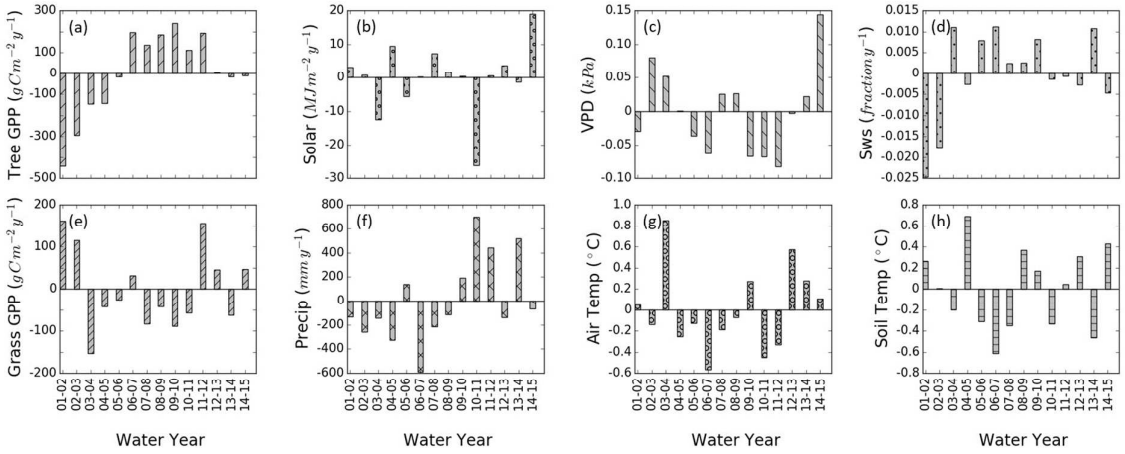

414

415 **Figure 5:** Anomaly plots for tree (a) and grass (e) GPP, plus solar radiation (Solar, b), vapour

416 pressure deficit (VPD, c), soil water storage (Sws, d), rainfall (Precip, f) and air (Ta, g)

417 and soil (Ts, h) temperature for the Howard Springs savanna site.

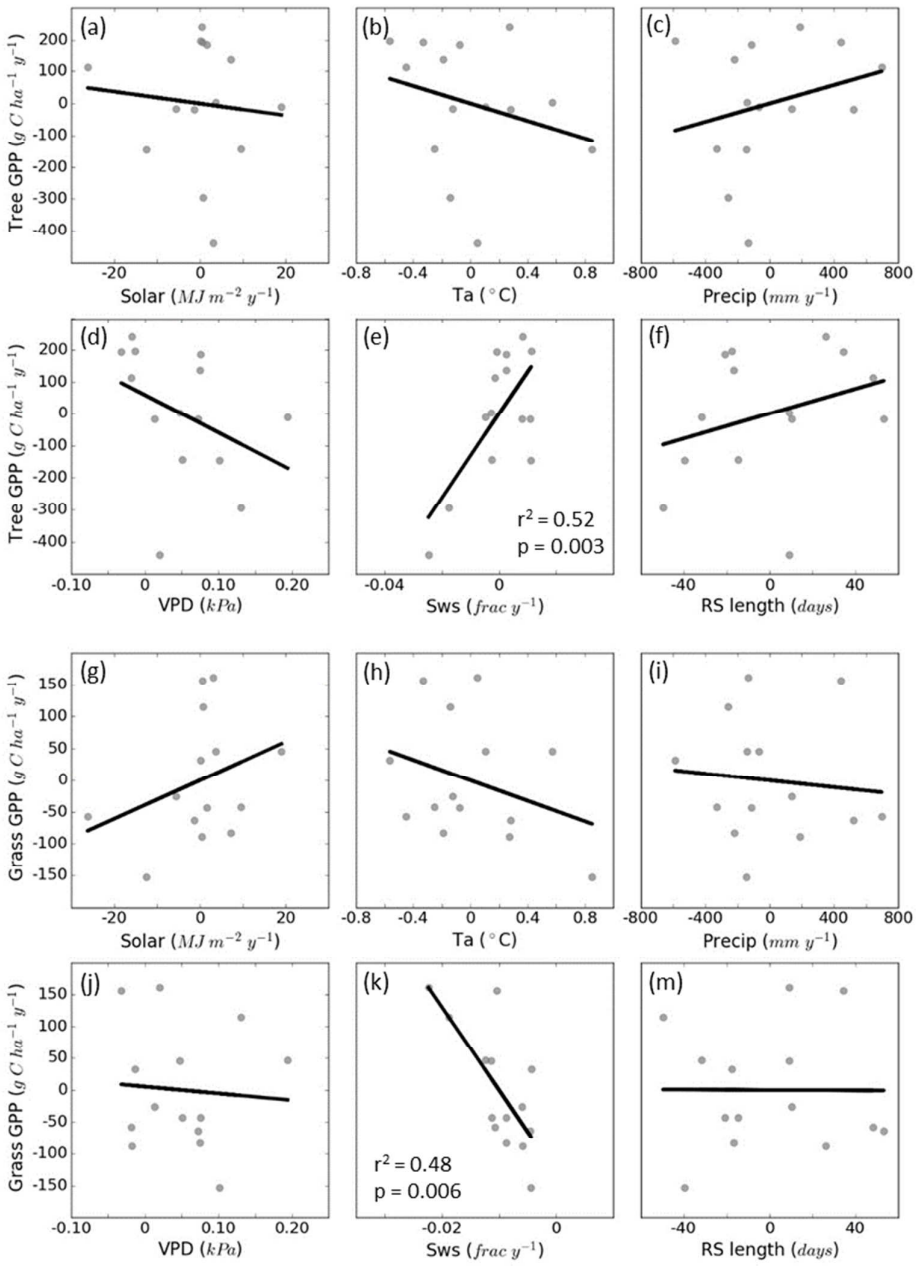

418

419 **Figure 6:** Linear regression relationships of yearly solar radiation (Solar, a & g), air
420 temperature (Ta, b & h) rainfall (Precip, c & i), vapour pressure deficit (VPD, d & j)
421 soil water storage (Sws, e & k) and rainy season (RS, f & m) length anomalies against
422 tree and grass gross primary productivity (GPP) anomalies for the Howard Springs
423 site from 2001 to 2015. Anomalies represent the change from the 2001-2015 mean,

based on water-years (i.e. Jul-Jun). Only significant anomaly correlations are given, as indicated on the plots by r^2 values and p values of <0.05 as a sign of statistical significant.

Variability in the tree-grass GPP ratio at Howard Springs

Under enhanced atmospheric CO_2 levels, woody thickening is likely to increase the tree-grass GPP ratio in savannas. To determine if woody thickening was occurring at Howard Springs, we calculated yearly sums of tree and grass GPP, as well as the tree-grass GPP ratio anomaly (Fig. 7). In general, over the first half of the period there was a slight increasing trend in tree GPP and a decrease in the grasses, which translated into an increase in the tree-grass GPP ratio up to 2010-2011. However, after this point, the tree-grass GPP ratio decreased (Fig. 7), with the overall result that there was no significant ($p = 0.18$) linear trend over time that would be consistent with woody thickening. As such, we cannot conclude from this dataset that woody thickening occurred at Howard Springs during this time.

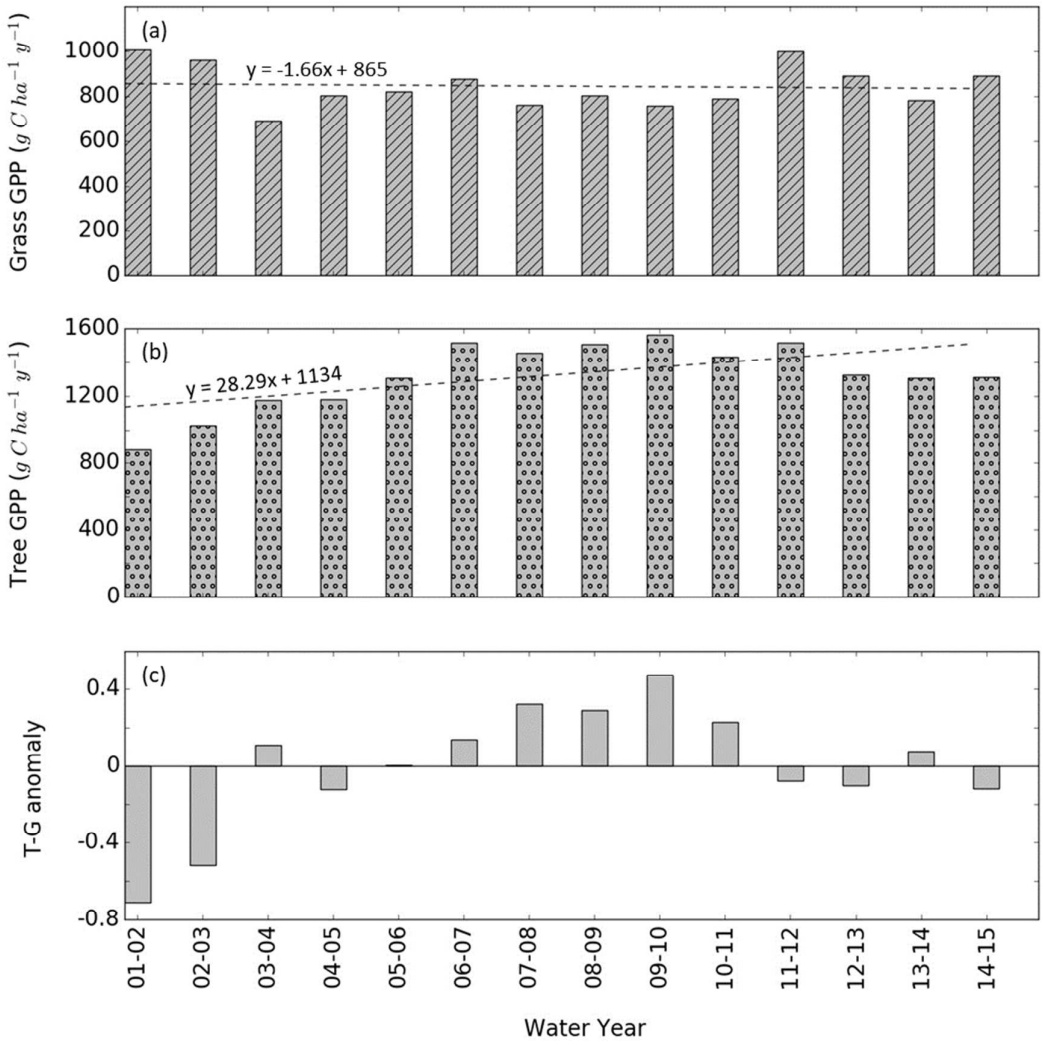

439

440 **Figure 7:** Annual model estimates for grass (a) and tree (b) gross primary productivity (GPP),
441 as well as the tree-grass GPP ratio anomaly (c), for the Howard Springs savanna from
442 the water-year (i.e. Jul-Jun) 2001-2002 to 2014-2015. Each plot also shows the trend
443 in growth over the study period.

444

445 Despite the apparent lack of woody thickening at Howard Springs, there was still a distinct
446 cyclical pattern in the tree-grass GPP ratio anomaly over time (Fig. 7; c) that could be

447 correlated with modes of climate variability. Recent work from Rogers & Beringer, (2016)
448 showed that IAV in rainfall for the Howard Springs region was correlated most strongly with
449 changes in the SOI, the TSI and the II. Therefore, we used these in conjunction with a
450 measure of the AUSMI to test the level of influence of the Australian monsoon on inter-
451 annual tree and grass productivity. This analysis revealed that of the four indices, the SOI had
452 a significant relationship with the tree-grass anomaly (Fig. 8) only if the level of significance
453 was relaxed to $p = 0.10$ (instead of $p = 0.05$). In general, for years when the SOI had a
454 positive value, the tree-grass anomaly was also positive, indicating a benefit to the trees over
455 the grasses. During years where the SOI was negative overall, the grasses benefited, as shown
456 by negative tree-grass anomaly values (Fig. 8).

457

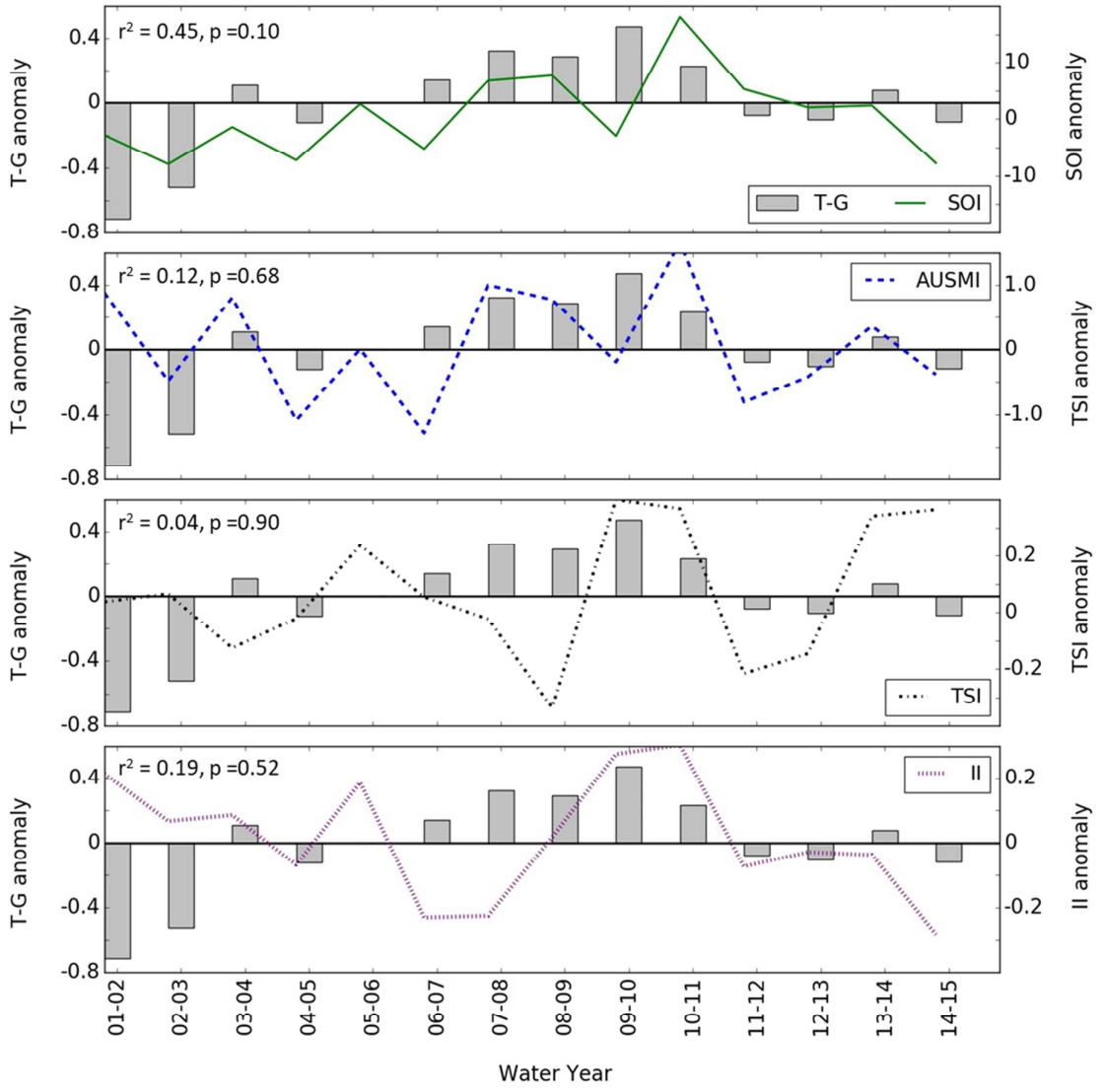

458

459 **Figure 8:** Time series plots of the yearly Howard Springs tree-grass anomaly against four key
460 climate indices found to influence long-term precipitation at Howard Springs (Rogers
461 & Beringer, 2017). These indices include the Southern Oscillation Index (SOI), the
462 Australian Monsoon Index (AUSMI), the Tasman Sea Index (TSI) and the Indonesia
463 Index (II). Correlation between each climate index and the tree-grass anomaly are
464 given by the r^2 values and its level of significance is given by the p-values.

465

466

Discussion

We have shown how tree and grass productivity varies over the long-term in an Australian tropical savanna and what the primary meteorological factors are that determine this variability, both seasonally and inter-annually. Both tree and grass GPP of this savanna were light limited during the wet season and water limited during the dry season. Whitley et al., (2011) concluded that mesic (high rainfall) savannas, such as Howard Springs, were light limited in the wet season due to a limited capacity of the vegetation to absorb light under ample soil water conditions, and in the dry season due to loss of canopy leaf area. Thick cloud cover during the wet season, from the summer monsoon, can also reduce productivity due to significant reductions in the quantity of total radiation (direct and diffuse) reaching the land surface (Kanniah, Beringer, & Hutley, 2013). The summer monsoon is most active from Dec-Mar (Cook & Heerdegen, 2001), which is when solar radiation limits tree and grass productivity the most (Fig. 4). These studies highlight the complex way in which savanna vegetation has adapted to its climatic range, as well as how it responds to inter-annual climatic variability.

At the onset of the dry season the annual C_4 grasses senesce (Andrew & Mott, 1983; Moore et al., 2017), leaving perennial C_4 grasses and woody understory species to contribute towards GPP in the understory (Moore et al., 2016, 2017). These species rely on moisture available in the surface soil layers to remain productive (Prior, Eamus, & Duff, 1997; Werner & Prior, 2013) and are often dormant during the late dry season when these layers are depleted (Prior et al., 2006; Werner & Prior, 2013). Likewise, the overstory tree species also maximise their usage of surface soil moisture while moisture remains available in the early dry season (Cook et al., 1998; Werner & Murphy, 2001). However, the trees also have an extensive root system that gives them access to this deeper water during the dry season (Cook et al., 1998; Eamus, Chen, Kelley, & Hutley, 2002; Kelley, O'Grady, Hutley, & Eamus, 2007;

492 Walker & Langridge, 1997), and they are able to maintain a nearly constant transpiration rate
493 year-round (Hutley, O'Grady, & Eamus, 2000; O'Grady, Eamus, & Hutley, 1999). At the
494 ecosystem scale, O'Grady, Eamus, & Hutley, (1999) found a strong coupling between tree
495 water use and VPD, particularly during the late dry season when atmospheric VPD is at its
496 highest, showing that the trees are limited in their ability to maintain stomatal closure. In our
497 analysis, we found that VPD also increased slightly in importance during the late dry season
498 (Aug-Oct) for the grasses, even though Sws at 100 cm remained the most important variable
499 overall (Fig. 4). This result is consistent with the findings of Walker & Langridge, (1997)
500 who concluded sub-soil moisture status has a significant influence on productivity in these
501 savannas.

502 In addition to investment in deeper roots, most tree species reduce their foliage cover in order
503 to maintain transpiration rates as soil water availability declines (Hutley, O'Grady, & Eamus,
504 2000; O'Grady, Eamus, & Hutley, 1999), which also reduces productivity by the late dry
505 season (Eamus, Myers, Duff, & Williams, 1999; Prior, Eamus, & Duff, 1997). Decreasing
506 soil water availability triggers the trees to regulate when and for how long their leaf stomata
507 are open to reduce water loss (Eamus & Cole, 1997; Prior, Eamus, & Duff, 1997). However,
508 as demonstrated by Myers, Williams, Fordyce, Duff, & Eamus, (1998) in an early dry season
509 irrigation experiment, the trees can retain leaves, providing more photosynthetic structures
510 that facilitate high rates of productivity in the dry season. The adaptive capacity of the trees
511 to resource availability provides a likely explanation for why there was a positive correlation
512 between increasing soil water availability and tree productivity (Fig. 6). While our analysis
513 could be improved by the inclusion of deeper Sws monitoring (if available), we have shown
514 the importance of soil moisture as a driver of tree-grass productivity both inter-annually and
515 during the dry season, with increasing importance for deep soil moisture as the dry season
516 progresses.

517 Another important question surrounding the future of savannas is how the tree-grass GPP
518 ratio is likely to change as atmospheric CO_2 levels continue to increase (Scheiter & Higgins,
519 2009; Scheiter, Higgins, Beringer, & Hutley, 2015). While our study revealed no significant
520 change in the tree-grass GPP ratio, a recent analysis of tree increment (i.e. from 2008 to 2014)
521 at Howard Springs showed a biomass increase of 0.5 t C ha^{-1} y^{-1} (Rudge, 2015). This is at the
522 upper end of reported tree growth for north Australian savannas (Beringer, Hutley, Tapper, &
523 Cernusak, 2007; Cook et al., 2005; Lehmann, Prior, & Bowman, 2009; Murphy, Lehmann,
524 Russell-Smith, & Lawes, 2014) and is consistent with reported site net ecosystem
525 productivity (Beringer et al., 2016), site disturbance history and increasing site rainfall
526 (Hutley & Beringer, 2010). A key finding of Rudge (2015) was that increasing biomass
527 primarily occurred in the middle to high tree size classes and that there was little change in
528 size class distribution (i.e. no juvenile recruitment). Therefore, woody thickening is not
529 significant at Howard Springs. The work of Rudge (2015) shows that biomass is being
530 accumulated at a slow rate, but that it is due to the growth of individual trees, rather than the
531 recruitment (i.e. thickening) of saplings. This is consistent with our finding that there is no
532 temporal trend of changing tree-grass GPP ratio over the past 15 years at Howard Springs
533 (Figure 7; c).

534 Varying degrees of woody thickening have been detected at other sites in the Northern
535 Territory savannas, including in the Kakadu (Bowman, Riley, Boggs, Lehmann, & Prior,
536 2008) and Litchfield (Bowman, Walsh, & Milne, 2001) national parks. Spatial variability in
537 thickening is likely to be a long-term response to fire management in the Australian savanna
538 region, which is highly heterogeneous (Beringer et al., 2015; Scheiter, Higgins, Beringer, &
539 Hutley, 2015). The Howard Springs site is intensively managed each year with control
540 burning to reduce the threat of high intensity, late dry season fires damaging the eddy
541 covariance equipment. However, late dry season fires are a common occurrence in the

Howard Springs region (return rates of 1-3 years (Beringer et al., 2015)) as it is located approximately 5 km from a low density peri-urban development (Fig. 1; a) and receives little management from local fire authorities (Russell-Smith et al., 2013; Russell-Smith et al., 2003). These high intensity fires do encroach upon the Howard Springs flux footprint, resulting in top-kill of juveniles that would limit woody thickening (Lawes, Richards, Dathe, & Midgley, 2011; Prior et al., 2006; Prior, Williams, & Bowman, 2010) at the site. This highlights the important role fire plays in shaping savanna ecosystem structure and supports the need for further research into how it may change in the future.

Along with fire, our study revealed the importance of the SOI as a driver of tree-grass productivity at Howard Springs (Fig. 7). The SOI provides an indication of El Niño/La Niña driven climatic variability that influences Ta and Fsd, as well as rainfall (Broich et al., 2014; Risbey, Pook, McIntosh, Wheeler, & Hendon, 2009). As such, it has been found to correlate with vegetation productivity (Nicholls, 1986, 1991) and phenology (Broich et al., 2014) for many regions of Australia. In the northern Australian savanna region, the SOI has also been correlated with fire activity (Harris, Tapper, Packham, Orlove, & Nicholls, 2008), which is linked with grass productivity in particular.

The 15-year flux record included a record breaking La Niña year (2010-2011), which resulted in a greening pulse over much of the terrestrial southern hemisphere (Ahlström et al., 2015; Poulter et al., 2014). This greening effect was strongly evident in xeric (low rainfall) savannas of inner continental Australia (Cleverly et al., 2016), and the mesic (higher rainfall) Howard Springs savanna also experienced its highest rainfall year and lowest total solar energy year (Fig. 5). However, the response of tree and grass GPP to this anomalous year was mixed, with higher than average (but not maximum) GPP experienced by the trees and lower than average GPP experienced by the grasses (Fig. 5). However, grass GPP was at its highest in the year following the La Niña event, indicating a lag in the response of the grasses to the

rainfall surplus. Recent work from Ma, Baldocchi, Wolf, & Verfaillie, (2016) showed a similar result in an oak-grass temperate savanna in California, with the research concluding that ecosystem-level responses of tree and grass GPP were driven by slow (i.e. often lagged) responses to meteorological variability. While xeric savannas have evolved to be fast responders to climatic pulses (Cleverly et al., 2016), our results indicate that mesic savannas might be slower at responding to similar climatic pulses. As models improve at capturing savanna productivity dynamics (Whitley et al., 2017), there will be more opportunities for exploring tree-grass responses to climate across the global savanna biome.

In summary, our findings suggest that mesic and xeric savanna ecosystems might respond very differently to climate driven changes in the timing and distribution of annual rainfall and how they relate to energy availability in the wet season and soil moisture availability in the dry season. This study fills an important gap in our understanding of the long-term tree and grass productivity dynamics of a tropical savanna. By identifying the importance of light availability in the wet season and soil moisture availability in the dry season, as well as the influence of inter-annual variability in soil moisture and climate indices (i.e. SOI), it puts us one step closer towards determining how the tree-grass dynamic may shift as the climate changes in the coming century.

Author Contributions

Field work and experimental design was executed by C. Moore, J. Beringer, L. Hutley and B. Evans. Data analysis was chiefly carried out by C. Moore. The DIFFUSE model analysis was provided by R. Donohue. Code for the Random Forest analysis was provided by J. Exbrayat. The manuscript was prepared by C. Moore with contributions from all co-authors.

Data Availability

All eddy covariance data used in this study are available for download from the OzFlux website (www.ozflux.org.au), under the TERN Attribution-Share Alike- Non Commercial (TERN BY-SA-NC) Data Licence v1.0. Climate index data are available from the websites as follows: TSI and II; http://climate-cms.unsw.wikispaces.net/ERA+INTERIM, SOI; http://www.bom.gov.au/climate/enso/soi_monthly.txt, AUSMI; http://apdrc.soest.hawaii.edu/projects/monsoon/ausmidx/ausmidx-djf.txt)

Acknowledgements

The authors would like to acknowledge support and funding from OzFlux and the overarching Terrestrial Ecosystem Research Network (TERN), which is supported by the Australian Government through the National Collaborative Research Infrastructure Strategy. This work utilised data collected by grants funded by the Australian Research Council (DP0344744, DP0772981 and DP130101566). J. Beringer is funded under an ARC FT (FT110100602). B. Evans is funded by the TERN Ecosystem Modelling and Scaling Infrastructure. Special thanks are also made to Dr. Peter Isaac for his development of the OzFluxQC standardised processing tools, to Mr. Matthew Northwood for all his efforts in maintaining the Howard Springs site and to Ms. Cassandra Rogers for her help with interpreting the climate indices used in this research.

References

Ahlström, A., Raupach, M. R., Schurgers, G., Smith, B., Arneth, A., Jung, M., … Zeng, N. (2015). The dominant role of semi-arid ecosystems in the trend and variability of the land CO2 sink. *Science*, *348*(6237), 895 LP-899. https://doi.org/10.1126/science.aaa1668

Andrew, M. H., & Mott, J. J. (1983). Annuals with transient seed banks: the population biology of indigenous Sorghum species of tropical north-west Australia. *Australian Journal of Ecology*, *8*(3), 265–276. https://doi.org/10.1111/j.1442-9993.1983.tb01324.x

Beer, C., Reichstein, M., Tomelleri, E., Ciais, P., Jung, M., Carvalhais, N., … Papale, D. (2010). Terrestrial gross carbon dioxide uptake: Global distribution and covariation with climate. *Science*, *329*(5993), 834–838. https://doi.org/10.1126/science.1184984

Beerling, D. J., & Osborne, C. P. (2006). The origin of the savanna biome. *Global Change Biology*, *12*(11), 2023–2031. https://doi.org/10.1111/j.1365-2486.2006.01239.x

Beringer, J., Hacker, J., Hutley, L. B., Leuning, R., Arndt, S. K., Amiri, R., … Zegelin, S. (2011). Special - Savanna patterns of energy and carbon integrated across the landscape. *Bulletin of the American Meteorological Society*, *92*(11), 1467–1485. https://doi.org/10.1175/2011BAMS2948.1

Beringer, J., Hutley, L. B., Abramson, D., Arndt, S. K., Briggs, P., Bristow, M., … Uotila, P. (2015). Fire in Australian savannas: From leaf to landscape. *Global Change Biology*, *21*(1), 62–81. https://doi.org/10.1111/gcb.12686

Beringer, J., Hutley, L. B., Tapper, N. J., & Cernusak, L. A. (2007). Savanna fires and their

638 impact on net ecosystem productivity in North Australia. *Global Change Biology*, *13*(5),
639 990–1004. https://doi.org/10.1111/j.1365-2486.2007.01334.x
640 Beringer, J., Hutley, L. B., Tapper, N. J., Coutts, A., Kerley, A., & O'Grady, A. P. (2003).
641 Fire impacts on surface heat, moisture and carbon fluxes from a tropical savanna in
642 northern Australia. *International Journal of Wildland Fire*, *12*, 333.
643 https://doi.org/10.1071/WF03023
644 Beringer, J., Hutley, L., McHugh, I., Arndt, S., Campbell, D., Cleugh, H., … Wardlaw, T.
645 (2016). An introduction to the Australian and New Zealand flux tower network - OzFlux.
646 *Biogeosciences*. https://doi.org/10.5194/bg-13-5895-2016
647 Beringer, J., Mchugh, I., Hutley, L. B., Isaac, P., & Kljun, N. (2017). Technical note :
648 Dynamic INtegrated Gap-filling and partitioning for OzFlux (DINGO), *Biogeosciences*,
649 1457–1460. https://doi.org/10.5194/bg-14-1457-2017
650 Bonan, G. B. (2008). *Ecological Climatology: Concepts and Applications* (2nd Ed.). New
651 York: Cambridge University Press.
652 Bond, W. J., & Keeley, J. E. (2005). Fire as a global "herbivore": The ecology and evolution
653 of flammable ecosystems. *Trends in Ecology and Evolution*, *20*(7), 387–394.
654 https://doi.org/10.1016/j.tree.2005.04.025
655 Bowman, D. M. J. S., Brown, G. K., Braby, M. F., Brown, J. R., Cook, L. G., Crisp, M.
656 D., … Ladiges, P. Y. (2010). Biogeography of the Australian monsoon tropics. *Journal*
657 *of Biogeography*, *37*(2), 201–216. https://doi.org/10.1111/j.1365-2699.2009.02210.x
658 Bowman, D. M. J. S., Riley, J. E., Boggs, G. S., Lehmann, C. E. R., & Prior, L. D. (2008).
659 Do feral buffalo (Bubalus bubalis) explain the increase of woody cover in savannas of
660 Kakadu National Park, Australia? *Journal of Biogeography*, *35*(11), 1976–1988.
661 https://doi.org/10.1111/j.1365-2699.2008.01934.x
662 Bowman, D. M. J. S., Walsh, A., & Milne, D. J. (2001). Forest expansion and grassland

663 contraction within a Eucalyptus savanna matrix between 1941 and 1994 at Litchfield
664 National Park in the Australian monsoon tropics. *Global Ecology and Biogeography*,
665 *10*(5), 535–548. https://doi.org/10.1046/j.1466-822x.2001.00252.x
666 Breiman, L. (2001). Random Forests. *Machine Learning*, *45*, 5–32.
667 Bristow, M., Hutley, L. B., Beringer, J., Livesley, S. J., Edwards, A. C., & Arndt, S. K.
668 (2016). Quantifying the relative importance of greenhouse gas emissions from current
669 and future savanna land use change across northern Australia. *Biogeosciences*, *13*,
670 6285–6303. https://doi.org/10.5194/bg-13-6285-2016
671 Broich, M., Huete, A., Tulbure, M. G., Ma, X., Xin, Q., Paget, M., … Held, A. (2014). Land
672 surface phenological response to decadal climate variability across Australia using
673 satellite remote sensing. *Biogeosciences*, *11*(18), 5181–5198. https://doi.org/10.5194/bg-
674 11-5181-2014
675 Browning, D. M., Archer, S. R., Asner, G. P., McClaran, M. P., & Wessman, C. A. (2008).
676 Woody plants in grasslands: Post-encroachment stand dynamics. *Ecological*
677 *Applications*, *18*(4), 928–944. https://doi.org/10.1890/07-1559.1
678 Cernusak, L. A., Hutley, L. B., Beringer, J., Holtum, J. A. M., & Turner, B. L. (2011).
679 Photosynthetic physiology of eucalypts along a sub-continental rainfall gradient in
680 northern Australia. *Agricultural and Forest Meteorology*, *151*(11), 1462–1470.
681 https://doi.org/10.1016/j.agrformet.2011.01.006
682 Chapin III, F. S., Matson, P. A., & Vitousek, P. (2011). *Principles of terrestrial ecosystem*
683 *ecology* (2nd Ed.). New York: Springer.
684 Cleverly, J., Eamus, D., Van Gorsel, E., Chen, C., Rumman, R., Luo, Q., … Huete, A. (2016).
685 Productivity and evapotranspiration of two contrasting semiarid ecosystems following
686 the 2011 global carbon land sink anomaly. *Agricultural and Forest Meteorology*, *220*,
687 151–159. https://doi.org/10.1016/j.agrformet.2016.01.086

688 Cook, G. D., & Heerdegen, R. G. (2001). Spatial variation in the duration of the rainy season
689 in monsoonal Australia. *International Journal of Climatology*, *21*(14), 1723–1732.
690 https://doi.org/10.1002/joc.704
691 Cook, G. D., Liedloff, A. C., Eager, R. W., Chen, X., Williams, R. J., O'Grady, A. P., &
692 Hutley, L. B. (2005). The estimation of carbon budgets of frequently burnt tree stands in
693 savannas of northern Australia, using allometric analysis and isotopic discrimination.
694 *Australian Journal of Botany*, *53*(7), 621–630. https://doi.org/10.1071/BT04150
695 Cook, P. G., Hatton, T. J., Pidsley, D., Herczeg, A. L., Held, A., O'Grady, A., & Eamus, D.
696 (1998). Water balance of a tropical woodland ecosystem, Northern Australia: A
697 combination of micro-meteorological, soil physical and groundwater chemical
698 approaches. *Journal of Hydrology*, *210*(1–4), 161–177.
699 Donohue, R. J., Hume, I. H., Roderick, M. L., McVicar, T. R., Beringer, J., Hutley, L. B., …
700 Arndt, S. K. (2014). Evaluation of the remote-sensing-based DIFFUSE model for
701 estimating photosynthesis of vegetation. *Remote Sensing of Environment*, *155*, 349–365.
702 https://doi.org/10.1016/j.rse.2014.09.007
703 Donohue, R. J., McVicar, T. R., & Roderick, M. L. (2009). Climate-related trends in
704 Australian vegetation cover as inferred from satellite observations, 1981-2006. *Global*
705 *Change Biology*, *15*(4), 1025–1039. https://doi.org/10.1111/j.1365-2486.2008.01746.x
706 Donohue, R. J., McVicar, T. R., & Roderick, M. L. (2010). Assessing the ability of potential
707 evaporation formulations to capture the dynamics in evaporative demand within a
708 changing climate. *Journal of Hydrology*, *386*(1–4), 186–197.
709 https://doi.org/10.1016/j.jhydrol.2010.03.020
710 Donohue, R. J., Roderick, M. L., McVicar, T. R., & Farquhar, G. D. (2013). Impact of CO2
711 fertilization on maximum foliage cover across the globe's warm, arid environments.
712 *Geophysical Research Letters*, *40*(12), 3031–3035. https://doi.org/10.1002/grl.50563

713 Duff, G. A., Myers, B. A., Williams, R. J., Eamus, D., O'Grady, A., & Fordyce, I. R. (1997).
714 Seasonal patterns in soil moisture, vapour pressure deficit, tree canopy cover and pre-
715 dawn water potential in a Northern Australian savanna. *Australian Journal of Botany*,
716 *45*(2), 211–224.
717 Dyer, R., & Smith, M. S. (2003). Ecological and economic assessment of prescribed burning
718 impacts in semi-arid pastoral lands of northern Australia. *International Journal of*
719 *Wildland Fire*, *12*(3–4), 403–413.
720 Eamus, D., Chen, X., Kelley, G., & Hutley, L. B. (2002). Root biomass and root fractal
721 analyses of an open Eucalyptus forest in a savanna of north Australia. *Australian*
722 *Journal of Botany*, *50*(1), 31–41. https://doi.org/10.1071/BT01054
723 Eamus, D., & Cole, S. (1997). Diurnal and seasonal comparisons of assimilation, phyllode
724 conductance and water potential of three Acacia and one Eucalyptus species in the wet–
725 dry tropics of …. *Australian Journal of Botany*, *45*, 275–290. https://doi.org/Doi
726 10.1071/Bt96020
727 Eamus, D., Hutley, L. B., & O'Grady, A. P. (2001). Daily and seasonal patterns of carbon
728 and water fluxes above a north Australian savanna. *Tree Physiology*, *21*(12–13), 977–
729 988.
730 Eamus, D., Myers, B., Duff, G., & Williams, D. (1999). Seasonal changes in photosynthesis
731 of eight savanna tree species. *Tree Physiology*, *19*(10), 665–671.
732 Eamus, D., & Prior, L. (2001). Ecophysiology of trees of seasonally dry tropics: Comparisons
733 among phenologies. *Advances in Ecological Research*.
734 Exbrayat, J. F., & Williams, M. (2015). Quantifying the net contribution of the historical
735 Amazonian deforestation to climate change. *Geophysical Research Letters*, *42*(8), 2968–
736 2976. https://doi.org/10.1002/2015GL063497
737 Field, C. B., Lobell, D. B., Peters, H. A., & Chiariello, N. R. (2007). Feedbacks of terrestrial

738 ecosystems to climate change. *Annual Review of Environmental Resources*, *32*, 1–29.
739 https://doi.org/10.1146/annurev.energy.32.053006.141119
740 Friedl, M. A., Mciver, D. K., Hodges, J. C. F., Zhang, X. Y., Muchoney, D., & Strahler, A. H.
741 (2002). Global land cover mapping from MODIS : algorithms and early results. *Remote*
742 *Sensing of Environment*, *83*, 287–302.
743 Gibson, H. S. (2015). IGBP MODIS Land Cover 500m Annual. United Kingdom:
744 Department of Zoology, University of Oxford. Retrieved from
745 http://www.map.ox.ac.uk/map-earth-engine-meta-data/
746 Gill, T. K., Armston, J. D., Phinn, S. R., & Pailthorpe, B. A. (2006). A comparison of
747 MODIS time-series decomposition methods for estimating evergreen foliage cover. In
748 *13th Australasian Remote Sensing & Photogrammerty Conference: Canberra*.
749 Grace, J., José, J. S., Meir, P., Miranda, H. S., & Montes, R. A. (2006). Productivity and
750 carbon fluxes of tropical savannas. *Journal of Biogeography*, *33*(3), 387–400.
751 https://doi.org/10.1111/j.1365-2699.2005.01448.x
752 Harris, S., Tapper, N., Packham, D., Orlove, B., & Nicholls, N. (2008). The relationship
753 between the monsoonal summer rain and dry-season fire activity of northern Australia.
754 *International Journal of Wildland Fire*, *17*(5), 674–684.
755 https://doi.org/10.1071/WF06160
756 Higgins, S. I., & Scheiter, S. (2012). Atmospheric CO 2 forces abrupt vegetation shifts
757 locally, but not globally. *Nature*, *488*(7410), 209–212.
758 https://doi.org/10.1038/nature11238
759 Hutley, L. B., & Beringer, J. (2010). Disturbance and climatic drivers of carbon dynamics of
760 a northern Australian tropical savanna . In M. J. Hill & N. P. Hanan (Eds.), *Ecosystem*
761 *Function in Savannas: Measurement and Modelling at Landscape and Global Scales* .
762 Florida: CRC Press.

763 Hutley, L. B., Beringer, J., Isaac, P. R., Hacker, J. M., & Cernusak, L. A. (2011). A sub-
764 continental scale living laboratory: Spatial patterns of savanna vegetation over a rainfall
765 gradient in northern Australia. *Agricultural and Forest Meteorology*, *151*(11), 1417–
766 1428. https://doi.org/10.1016/j.agrformet.2011.03.002
767 Hutley, L. B., Evans, B. J., Beringer, J., Cook, G. D., Maier, S. W., & Razon, E. (2013).
768 Impacts of an extreme cyclone event on landscape-scale savanna fire, productivity and
769 greenhouse gas emissions. *Environmental Research Letters*, *8*(4), 1–12.
770 https://doi.org/10.1088/1748-9326/8/4/045023
771 Hutley, L. B., O'Grady, A. P., & Eamus, D. (2000). Evapotranspiration from eucalypt open-
772 forest savanna of northern australia. *Functional Ecology*, *14*(2), 183–194.
773 https://doi.org/10.1046/j.1365-2435.2000.00416.x
774 Isaac, P., Cleverly, J., McHugh, I., van Gorsel, E., Ewenz, C., & Beringer, J. (2017). OzFlux
775 Data: Network integration from collection to curation. *Biogeosciences*, *14*, 1–41.
776 https://doi.org/10.5194/bg-14-2903-2017
777 Isbell, R. F. (1996). *The Australian Soil Classification*. Collingwood, VIC: CSIRO
778 Publishing.
779 Kajikawa, Y., Wang, B., & Yang, J. (2010). A multi-time scale Australian monsoon index.
780 *International Journal of Climatology*, *30*(8), 1114–1120.
781 https://doi.org/10.1002/joc.1955
782 Kanniah, K. D., Beringer, J., & Hutley, L. (2013). Exploring the link between clouds,
783 radiation, and canopy productivity of tropical savannas. *Agricultural and Forest*
784 *Meteorology*, *182–183*, 304–313. https://doi.org/10.1016/j.agrformet.2013.06.010
785 Kanniah, K. D., Beringer, J., & Hutley, L. B. (2010). The comparative role of key
786 environmental factors in determining savanna productivity and carbon fluxes: A review,
787 with special reference to Northern Australia. *Progress in Physical Geography*, *34*(4),

459–490. https://doi.org/10.1177/0309133310364933

Kanniah, K. D., Beringer, J., & Hutley, L. B. (2011). Environmental controls on the spatial variability of savanna productivity in the Northern Territory, Australia. *Agricultural and Forest Meteorology*, *151*(11), 1429–1439. https://doi.org/10.1016/j.agrformet.2011.06.009

Kelley, G., O'Grady, A. P., Hutley, L. B., & Eamus, D. (2007). A comparison of tree water use in two contiguous vegetation communities of the seasonally dry tropics of northern Australia: The importance of site water budget to tree hydraulics. *Australian Journal of Botany*, *55*(7), 700–708. https://doi.org/10.1071/BT07021

Lawes, M. J., Richards, A., Dathe, J., & Midgley, J. J. (2011). Bark thickness determines fire resistance of selected tree species from fire-prone tropical savanna in north Australia. *Plant Ecology*, *212*(12), 2057–2069. https://doi.org/10.1007/s11258-011-9954-7

Lehmann, C. E. R., Prior, L. D., & Bowman, D. M. J. S. (2009). Fire controls population structure in four dominant tree species in a tropical savanna. *Oecologia*, *161*(3), 505–515. https://doi.org/10.1007/s00442-009-1395-9

Leuning, R., van Gorsel, E., Massman, W. J., & Isaac, P. R. (2012). Reflections on the surface energy imbalance problem. *Agricultural and Forest Meteorology*, *156*, 65–74. https://doi.org/10.1016/j.agrformet.2011.12.002

López-Blanco, E., Lund, M., Williams, M., Tamstorf, M. P., Westergaard-Nielsen, A., Exbrayat, J.-F., … Christensen, T. R. (2017). Exchange of CO2 in Arctic tundra : impacts of meteorological variations and biological disturbance. *Biogeosciences*, *14*, 4467–4483. https://doi.org/10.5194/bg-14-4467-2017

Ma, S., Baldocchi, D., Wolf, S., & Verfaillie, J. (2016). Slow ecosystem responses conditionally regulate annual carbon balance over 15 years in Californian oak-grass savanna. *Agricultural and Forest Meteorology*, *228–229*, 252–264.

https://doi.org/10.1016/j.agrformet.2016.07.016

Macinnis-Ng, C., Zeppel, M., Williams, M., & Eamus, D. (2011). Applying a SPA model to examine the impact of climate change on GPP of open woodlands and the potential for woody thickening. *Ecohydrology*, *379–393*, 379–393. https://doi.org/10.1002/eco.138

McHugh, I. D., Beringer, J., Cunningham, S. C., Baker, P. J., Cavagnaro, T. R., Nally, R. Mac, & Thompson, R. M. (2017). Interactions between nocturnal turbulent flux, storage and advection at an " ideal " eucalypt woodland site. *Biogeosciences*, 3027–3050. https://doi.org/10.5194/bg-14-3027-2017

Mistry, J. (2001). Savannas. *Progress in Physical Geography*, *25*(4), 552–559.

Monteith, J. L. (1972). Solar Radiation and Productivity in Tropical Ecosystems. *Journal of Applied Ecology*, *9*(3), 747–766. https://doi.org/10.2307/2401901

Moore, C. E., Beringer, J., Evans, B., Hutley, L. B., McHugh, I., & Tapper, N. J. (2016). The contribution of trees and grasses to productivity of an Australian tropical savanna. *Biogeosciences*, *13*, 2387–2403. https://doi.org/10.5194/bg-13-2387-2016

Moore, C. E., Beringer, J., Evans, B., Hutley, L. B., & Tapper, N. J. (2017). Tree-grass phenology information improves light use efficiency modelling of gross primary productivity for an Australian tropical savanna. *Biogeosciences*, *14*, 111–129. https://doi.org/10.5194/bg-14-111-2017

Murphy, B. F., & Timbal, B. (2008). A review of recent climate variability and climate change in Southeastern Australia. *International Journal of Climatology*, *28*(7), 859–879. https://doi.org/10.1002/joc.1627

Murphy, B. P., Lehmann, C. E. R., Russell-Smith, J., & Lawes, M. J. (2014). Fire regimes and woody biomass dynamics in Australian savannas. *Journal of Biogeography*, *41*(1), 133–144. https://doi.org/10.1111/jbi.12204

Murphy, B. P., Russell-Smith, J., & Prior, L. D. (2010). Frequent fires reduce tree growth in

northern Australian savannas: Implications for tree demography and carbon sequestration. *Global Change Biology*, *16*(1), 331–343. https://doi.org/10.1111/j.1365-2486.2009.01933.x

Myers, B. A, Williams, R. J., Fordyce, I., Duff, G. A, & Eamus, D. (1998). Does irrigation affect leaf phenology in deciduous and evergreen trees of the savannas of northern Australia? *Australian Journal of Ecology*, *23*(4), 329–339. https://doi.org/DOI 10.1111/j.1442-9993.1998.tb00738.x

Nicholls, N. (1986). Use of the Southern Oscillation to predict Australian sorghum yield. *Agricultural and Forest Meteorology*, *38*(1–3), 9–15. https://doi.org/10.1016/0168-1923(86)90046-8

Nicholls, N. (1989). Sea Surface Temperatures and Australian Winter Rainfall. *Journal of Climate*, *2*(9), 965–973. https://doi.org/10.1175/1520-0442(1989)002<0965:SSTAAW>2.0.CO;2

Nicholls, N. (1991). The El Niño/Southern Oscillation and Australian vegetation. *Vegetatio*, *91*(1–2), 23–36. https://doi.org/10.1007/BF00036045

O'Grady, A. P., Eamus, D., & Hutley, L. B. (1999). Transpiration increases during the dry season: patterns of tree water use in eucalypt open-forests of northern Australia. *Tree Physiology*, *19*(9), 591–597. https://doi.org/10.1093/treephys/19.9.591

Pedregosa, F., Varoquaux, G., Gramfort, A., Michel, V., Thirion, B., Grisel, O., … Duchesnay, É. (2011). Scikit-learn: Machine learning in Python. *Journal of Machine Learning Research*, *12*, 2825–2830.

Poulter, B., Frank, D., Ciais, P., Myneni, R. B., Andela, N., Bi, J., … van der Werf, G. R. (2014). Contribution of semi-arid ecosystems to interannual variability of the global carbon cycle. *Nature*, *509*(7502), 600–603. https://doi.org/10.1038/nature13376

Prior, L. D., Brook, B. W., Williams, R. J., Werner, P. A., Bradshaw, C. J. A., & Bowman, D.

M. J. S. (2006). Environmental and allometric drivers of tree growth rates in a north Australian savanna. *Forest Ecology and Management*, *234*(1–3), 164–180. https://doi.org/https://doi.org/10.1016/j.foreco.2006.06.034

Prior, L. D., Eamus, D., & Duff, G. A. (1997). Seasonal and diurnal patterns of carbon assimilation, stomatal conductance and leaf water potential in Eucalyptus tetrodonta saplings in a wet-dry savanna in northern australia. *Australian Journal of Botany*, *45*(2), 241–258.

Prior, L. D., Williams, R. J., & Bowman, D. M. J. S. (2010). Experimental evidence that fire causes a tree recruitment bottleneck in an Australian tropical savanna. *Journal of Tropical Ecology*, *26*(6), 595–603. https://doi.org/10.1017/S0266467410000362

Risbey, J. S., Pook, M. J., McIntosh, P. C., Wheeler, M. C., & Hendon, H. H. (2009). On the remote drivers of rainfall variability in Australia. *Monthly Weather Review*, *137*(10), 3233–3253. https://doi.org/10.1175/2009MWR2861.1

Roderick, M. L. (1999). Estimating the diffuse component from daily and monthly measurements of global radiation. *Agricultural and Forest Meteorology*, *95*(3), 169–185. https://doi.org/10.1016/S0168-1923(99)00028-3

Rogers, C., & Beringer, J. (2017). Describing rainfall in northern Australia using multiple climate indices. *Biogeosciences*, *14*, 597–615. https://doi.org/10.5194/bg-14-597-2017

Rudge, M. (2015). *Tree increment and fluvial export as carbon sink pathways in high rainfall savanna of north Australia*. *School of Environment*. Charles Darwin University, Darwin, NT, AUS.

Russell-Smith, J., Cook, G. D., Cooke, P. M., Edwards, A. C., Lendrum, M., Meyer, C. P., & Whitehead, P. J. (2013). Managing fire regimes in north Australian savannas: Applying Aboriginal approaches to contemporary global problems. *Frontiers in Ecology and the Environment*, *11*(SUPPL. 1), e55–e63. https://doi.org/10.1890/120251

888 Russell-Smith, J., Yates, C., Edwards, A., Allan, G. E., Cook, G. D., Cooke, P., … Smith, R.
889 (2003). Contemporary fire regimes of northern Australia, 1997–2001: change since
890 Aboriginal occupancy, challenges for sustainable management. *International Journal of*
891 *Wildland Fire*, *12*(4), 283. https://doi.org/10.1071/WF03015
892 Russell-Smith, J., & Yates, C. P. (2007). Australian savanna fire regimes: context, scales,
893 patchiness. *Fire Ecology*, *3*(1), 48–63.
894 Sage, R. F. (2004). The evolution of C4 photosynthesis. *New Phytologist*, *161*(2), 341–370.
895 https://doi.org/10.1111/j.1469-8137.2004.00974.x
896 Scheiter, S., & Higgins, S. I. (2009). Impacts of climate change on the vegetation of Africa:
897 An adaptive dynamic vegetation modelling approach. *Global Change Biology*, *15*(9),
898 2224–2246. https://doi.org/10.1111/j.1365-2486.2008.01838.x
899 Scheiter, S., Higgins, S. I., Beringer, J., & Hutley, L. B. (2015). Climate change and long-
900 term fire management impacts on Australian savannas. *The New Phytologist*, *205*(3),
901 1211–26. https://doi.org/10.1111/nph.13130
902 Schepen, A., Wang, Q. J., & Robertson, D. (2012). Evidence for using lagged climate indices
903 to forecast Australian seasonal rainfall. *Journal of Climate*, *25*(4), 1230–1246.
904 https://doi.org/10.1175/JCLI-D-11-00156.1
905 Scholes, R. J., & Archer, S. R. (1997). Tree-grass interactions in Savannas. *Annual Review of*
906 *Ecology and Systematics*, *28*, 517–544. https://doi.org/10.1146/annurev.ecolsys.28.1.517
907 Scurlock, J. M. O., & Hall, D. O. (1998). The global carbon sink: a grassland perspective.
908 *Global Change Biology*, *4*(2), 229–233. https://doi.org/10.1046/j.1365-
909 2486.1998.00151.x
910 Shackleton, S. E., Shackleton, C. M., Netshiluvhi, T. R., Geach, B. S., Ballance, A., &
911 Fairbanks, D. H. K. (2002). Use patterns and value of savanna resources in three rural
912 villages in South Africa. *Economic Botany*, *56*(2), 130–146.

913 Shi, Y., Matsunaga, T., Saito, M., Yamaguchi, Y., & Chen, X. (2015). Comparison of global
914 inventories of CO<inf>2</inf> emissions from biomass burning during 2002-2011
915 derived from multiple satellite products. *Environmental Pollution*, *206*, 479–487.
916 https://doi.org/10.1016/j.envpol.2015.08.009
917 Sturman, A. P., & Tapper, N. J. (2006). *The weather and climate of Australia and New*
918 *Zealand*. *The weather and climate of Australia and New Zealand* (2nd ed.). Melbourne,
919 AUS: Oxford University Press.
920 Suppiah, R., & Hennessy, K. J. (1996). Trends in the intensity and frequency of heavy
921 rainfall in tropical Australia and links with the Southern Oscillation. *Australian*
922 *Meteorological Magazine*, *45*(1), 1–17. https://doi.org/10.1002/(SICI)1097-
923 0088(199808)18:10<1141::AID-JOC286>3.0.CO;2-P
924 Van Der Werf, G. R., Randerson, J. T., Giglio, L., Collatz, G. J., Mu, M., Kasibhatla, P.
925 S., … Van Leeuwen, T. T. (2010). Global fire emissions and the contribution of
926 deforestation, savanna, forest, agricultural, and peat fires (1997-2009). *Atmospheric*
927 *Chemistry and Physics*, *10*(23), 11707–11735. https://doi.org/10.5194/acp-10-11707-
928 2010
929 van Oldenborgh, G., Collins, M., Arblaster, J., Christensen, J., Marotzke, J., Power, S., …
930 Zhou, T. (2013). *Annex I: Atlas of Global and Regional Climate Projections*. (T. F.
931 Stocker, D. Qin, G. K. Plattner, M. Tignor, S. K. Allen, J. Boschung, … P. M. Midgley,
932 Eds.), *Climate Change 2013: The Physical Science Basis. Contribution of Working*
933 *Group I to the Fifth Assessment Report of the Intergovernmental Panel on Climate*
934 *Change*. https://doi.org/10.1017/CBO9781107415324.029
935 Walker, B. H., & Langridge, J. L. (1997). Predicting savanna vegetation structure on the basis
936 of plant available moisture (PAM) and plant available nutrients (PAN): a case study
937 from Australia. *Journal of Biogeography*. https://doi.org/10.1046/j.1365-

938 2699.1997.00123.x
939 Walsh, D., Russell-Smith, J., & Cowley, R. (2014). Fire and carbon management in a
940 diversified north Australian rangelands economy: research, policy and implementation
941 challenges for northern Australia. *Rangeland Journal*, *36*(4), 313–322.
942 Werner, P. A., & Murphy, P. G. (2001). Size-specific biomass allocation and water content of
943 above- and belowground components of three Eucalyptus species in a northern
944 Australian savanna. *Australian Journal of Botany*, *49*(2), 155–167.
945 Werner, P. A., & Prior, L. D. (2013). Demography and growth of subadult savanna trees:
946 Interactions of life history, size, fire season, and grassy understory. *Ecological*
947 *Monographs*, *83*(1), 67–93. https://doi.org/10.1890/12-1153.1
948 Whitley, R., Beringer, J., Hutley, L. B., Abramowitz, G., Kauwe, M. G. De, Evans, B., …
949 Schymanski, S. J. (2017). Challenges and opportunities in land surface modelling of
950 savanna ecosystems, 4711–4732.
951 Whitley, R. J., Macinnis-Ng, C. M. O., Hutley, L. B., Beringer, J., Zeppel, M., Williams,
952 M., … Eamus, D. (2011). Is productivity of mesic savannas light limited or water
953 limited? Results of a simulation study. *Global Change Biology*, *17*(10), 3130–3149.
954 https://doi.org/10.1111/j.1365-2486.2011.02425.x
955 Williams, R. J., Myers, B. A., Muller, W. J., Duff, G. A., & Eamus, D. (1997). Leaf
956 phenology of woody species in a North Australian tropical savanna. *Ecology*, *78*(8),
957 2542–2558. https://doi.org/10.1890/0012-9658(1997)078[2542:LPOWSI]2.0.CO;2
958 Zhou, Q., Hill, M. J., Sun, Q., & Schaaf, C. B. (2016). Retrieving understorey dynamics in
959 the Australian tropical savannah from time series decomposition and linear unmixing of
960 MODIS data. *International Journal of Remote Sensing*, *37*(6), 1445–1475.
961 https://doi.org/10.1080/01431161.2016.1154224
962

963

964

Figure Captions

Figure 1: MODIS Land Cover Product (MCD12Q1) using the International Geosphere-Biosphere Program (IGBP) classification system for a) the Northern Territory in Australia, b) the northern-west region of the northern territory and c) the area directly surrounding the Howard Springs OzFlux tower, with individual pixel resolution of 500 m (produced in ArcMap v10.1 using MODIS Land Cover data from Gibson (2015).

Figure 2: Time series and regression comparison of Howard Springs flux tower and DIFFUSE model estimates ($Model_O$ = original model, $Model_A$ = adjusted model to include understory woody contributions) of gross primary productivity (GPP, g C m^{-2} d^{-1}) for understory (a) and overstory (b) from September 2012 to June 2015. Regression plots show the line of best fit (solid line), the 1:1 line (dashed line), and the linear regression equation for modelled GPP (GPP_M) predicting tower GPP (GPP_T).

Figure 3: Long-term (15 year) ecosystem (Eco) gross primary productivity (GPP) flux tower time series, the partitioned overstory (O/S) and understory (U/S) GPP, plus rainfall, for the Howard Springs savanna site. Data are shown as monthly sums.

Figure 4: Meteorological drivers of monthly understory and overstory gross primary productivity (GPP) from 2001 to 2015 (a & b) and 2008 to 2015 (c & d) at Howard Springs. Meteorological drivers include soil water storage at 10 cm (Sws), Sws at 100 cm (Sws100), air temperature (Ta), vapour pressure deficit (VPD) and incoming solar radiation (Fsd). The bottom panel begins in 2008 due to the installation of the 100 cm Sws sensor in that year.

Figure 5: Anomaly plots for overstory (O/S) and understory (U/S) GPP, plus solar radiation (Solar), vapour pressure deficit (VPD), soil water storage (Sws), rainfall (Precip) and air (Ta) and soil (Ts) temperature for the Howard Springs savanna site.

Figure 6: Linear regression relationships of yearly solar radiation (Solar), air temperature (Ta) rainfall (Precip), vapour pressure deficit (VPD) soil water storage (Sws) and rainy season (RS) length anomalies against overstory (O/S) and understory (U/S) gross primary productivity (GPP) anomalies for the Howard Springs site from 2001 to 2015. Anomalies represent the change from the 2001-2015 mean, based on water-years (i.e. Jul-Jun). Correlations are given by the r^2 values, where (+) values represent a benefit of the increasing meteorological variable and (-) values represent inhibition of the increasing meteorological variable to GPP. Correlation significance is given by the p value, where p values <0.05 are significant.

Figure 7: Annual gross primary productivity (GPP) sums for the understory (U/S) and overstory (O/S), as well as the tree-grass GPP ratio anomaly, for the Howard Springs savanna from the water-year (i.e. Jul-Jun) 2001-2002 to 2014-2015. Each plot also shows the trend in growth over the study period.

Figure 8: Time series plots of the yearly Howard Springs tree-grass anomaly against four key climate indices found to influence long-term precipitation at Howard Springs (Rogers and Beringer, 2016). These indices include the Southern Oscillation Index (SOI), the Australian Monsoon Index (AUSMI), the Tasman Sea Index (TSI) and the Indonesia Index (II). Correlation between each climate index and the tree-grass anomaly are given by the r^2 values and its level of significance is given by the p-values, with p <0.05 indicating a significant relationship.